1

Heating of the Solar Chromosphere

P. Ulmschneider, Univ. Heidelberg and W. Kalkofen, Harvard-Smithsonian Center for Astrophysics, date: 10 Jan. 2002

Abstract: Overlying the photosphere, the chromosphere is a layer which is dominated by mechanical heating and magnetic fields. By simulating the chromospheric line and continuum emission, empirical models can be constructed which allow to evaluate the energy balance. The zoo of possible heating processes are discussed and the search effort to identify the correct mechanisms. It is found that acoustic waves are the basic heating mechanism for non-magnetic, and magnetohydrodynamic tube waves for the magnetic regions of the chromosphere.

1.1 Introduction

At the start of a total solar eclipse when the photosphere has just vanished behind the rim of the Moon, the Fraunhofer spectrum changes abruptly from absorption to emission; it is referred to as a *flash spectrum*. After the fading of the weak metal lines, the spectrum is dominated by Balmer lines of hydrogen, the H and K lines of Ca II, and He lines, all emanating from a quickly vanishing layer, called *chromosphere*, which extends over only a few thousand km above the solar limb; the chromosphere is named after the intense red color of the Hα line at 6563 Å. A few seconds later the chromosphere disappears again and the *corona*, which extends to many solar radii, becomes visible.

Grotrian (1939) and Edlén (1941) were surprised to discover that the corona is extremely hot when they identified the red and green coronal emission lines as lines of Fe X and XIV, which are emitted by gas with temperatures of $1 - 2 \cdot 10^6$ K. The existence of intermediate temperatures

was shown by the OSO satellites in the 1960's, which observed the full sequence of ions, e.g., from O II to O VI in the UV, indicating regions with temperatures from 10^4 to 10^5 K.

Based on observations with the IUE and Einstein satellites launched in the late 1970's it was found that essentially all late-type stars, which have surface convection zones, have such hot chromospheric layers, where the temperature increases in the outward direction from low photospheric values to about 10^4 K. From the top of the chromosphere (in most stars) the temperature then rises rapidly through a thin region, the so-called *transition layer*, to coronal values. For the Sun, this entire temperature range of the chromosphere and corona is now well observed in the UV and XUV parts of the spectrum with the SOHO satellite, launched in 1995 (Fleck, Domingo & Poland 1995).

The quiet solar chromosphere, i.e., outside active regions, is bifurcated into magnetic network and internetwork chromosphere. The network is characterized by strong magnetic fields, which are organized in tubes of intense magnetic flux, where the field strength reaches 1500 Gauss in the photosphere (Stenflo 1994). The field makes a contribution to the pressure that can exceed that of the gas. These magnetic flux tubes expand exponentially in the upward direction exponentially, with the radius of a cylindrical flux tube growing with an e-folding distance of four times the pressure scale height. The filling factor of the network increases from 1% in the photosphere to 15% in the layers of formation of the emission features in the H and K lines (Foukal, SPD meeting 2000) and to 100% in the so-called *magnetic canopy*. The internetwork region the magnetic field is dynamically unimportant.

The network is brighter than the internetwork chromosphere. The intensity ratio depends on the criterion and the height where it is measured. A typical value for the average brightness ratio of network to internetwork is 1.27 for Ca II K line emission (Skumanich, Smythe & Frazier 1975). In the region of formation of the Lyman continuum in the upper chromosphere, the Skylab observations indicate a range of variation of the intensity by a factor of nearly 10, corresponding to a temperature variation of about 10% of the ambient value (e.g., Vernazza, Avrett & Loeser 1981).

The temperature structure of the chromosphere is described by empirical models of the brightness seen in chromospheric emission (see Figure 1.1, discussed in the next section). These models do not explicitly separate magnetic from nonmagnetic regions, but one may suppose that the coolest model refers mainly to the nonmagnetic chromosphere in the interior of supergranulation cells and the hottest gives greatest weight to the magnetic

network. Although modeling on the basis of brightness distributions does not guarantee that the various models describe physically connected regions, the deduction that the temperature profile implies a heating mechanism provides support for these models as physical models (see the section on Wave Heating).

A deduction from the similarity of the temperature structures (see Fig. 3 for models A - F of Fontenla, Avrett & Loeser 1993) is that the heating mechanisms in the magnetic and nonmagnetic media is essentially the same, i.e., the dissipation has properties that appear to be independent of the magnetic field, although this leaves open the question of the mode of energy transport to the point of dissipation.

1.2 Empirical chromosphere models

The structure of the quiet chromosphere can be described by empirical models that match predictions against observations of radiation from the Sun (Vernazza, Avrett & Loeser 1981, Avrett 1985; Fontenla, Avrett & Loeser 1993). For the construction, the temperature is adjusted until a satisfactory fit is achieved between observed and predicted radiation fields. The pressure distribution is then determined from the hydrostatic equilibrium equation, which also yields density and height, resulting in a model that gives temperature and pressure as functions of height. Because of the combination of empirical adjustments and the use of an equation such models are referred to as semiempirical. Figure 1.1 shows the average model of the quiet chromosphere, labeled VAL81-C, by Vernazza et al. (1981). From the determined temperature and pressure distribution using a multilevel atom radiative transfer code the radiation losses due to the lines and continua have been computed resulting in a total loss of $4.6 \cdot 10^6$ erg cm^{-2} s^{-1} (mainly by Ca II H+K+IRT and Mg II h+k lines), which needs to be balanced by mechanical heating.

The variation of the chromospheric emission over the solar surface was described in six brightness models by Vernazza et al. (1981). The deviation from the coolest to the hottest model from the average one, model C, is about 7% at the height of 1 Mm; and, at heights where the fractional ionization of hydrogen is 10%, the temperature departs by maximally 4% from that of the average model.

Andersen & Athay (1989) analyzed the temperature structure of model C and found that Fe II lines are additional strong emitters which raise the total chromospheric radiation loss to $1.4 \cdot 10^7$ erg cm^{-2} s^{-1}. In addition the cooling rate per unit mass increases from a low value in the photosphere

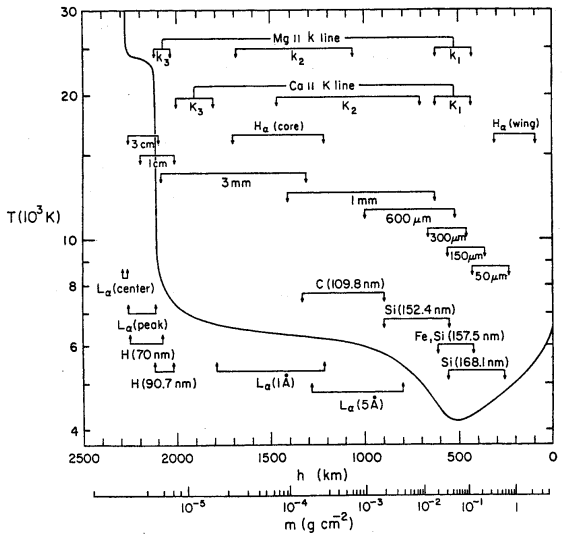

Fig. 1.1. The average model of the quiet solar chromosphere, VAL81-C, from Vernazza et al. (1981).

to practically a constant value in the temperature plateau region between 1 Mm and 2 Mm. Since heat conduction is negligible the energy that is radiated away must be delivered by a transport and dissipation mechanism to the point of emission. Consequently, the heating mechanism must have a dissipation rate per gram that increases from negligible values in the photosphere to a constant and high value in the region of the temperature plateau above 1 Mm.

1.3 Energy balance and the necessity of mechanical heating

To understand the chromospheric energy balance consider a gas element. An amount of heat dQ (erg cm^{-3}) flowing into the element across its boundaries raises the entropy S (erg g^{-1}K^{-1}) by

$$dS = \frac{dQ}{\rho T} \quad , \tag{1.1}$$

where T is the temperature and ρ the density. The thermodynamic variable entropy is used here because it has a bookkeeping quality for monitoring the energy flows in and out of the gas element. In adiabatic cases no energy flows occur, while rising S indicates that energy enters into the element. For a gas element moving with wind velocity v through the chromosphere one

can write an entropy conservation equation (in the Lagrange frame)

$$\frac{dS}{dt} = \frac{\partial S}{\partial t} + v\frac{\partial S}{\partial z} = \left.\frac{dS}{dt}\right|_R + \left.\frac{dS}{dt}\right|_J + \left.\frac{dS}{dt}\right|_C + \left.\frac{dS}{dt}\right|_V + \left.\frac{dS}{dt}\right|_M \quad . \tag{1.2}$$

Here t is time and z is height in a plane-parallel atmosphere. The five terms on the right hand side are called radiative, Joule, thermal conductive and viscous and mechanical heating. Mechanical heating denotes all processes which convert nonradiative, nonconductive, hydrodynamic or magnetic energy propagating through the gas element into heat (microscopic random thermal motion).

Let us estimate the rough sizes of the individual heating terms in Eq. (1.2). Consider a typical acoustic or magnetohydrodynamic (MHD) disturbance in the solar chromosphere with characteristic perturbations of size $L = 200\ km$, temperature $\Delta T = 1000\ K$, velocity $\Delta v = 3\ km/s$ and magnetic field $\Delta B = 10\ G$. Using appropriate values for the thermal conductivity $\kappa_{th} = 10^5\ erg\ cm^{-1}s^{-1}K^{-1}$, viscosity $\eta_{vis} = 5 \cdot 10^{-4}\ dyn\ s\ cm^{-2}$ and electrical conductivity $\lambda_{el} = 2 \cdot 10^{10}\ s^{-1}$ we find for the *thermal conductive heating rate* ($erg\ cm^{-3}s^{-1}$)

$$\Phi_C = \rho T \left.\frac{dS}{dt}\right|_C = \frac{d}{dz}\kappa_{th}\frac{dT}{dz} \approx \frac{\kappa_{th}\Delta T}{L^2} \approx 3 \cdot 10^{-7} \quad , \tag{1.3}$$

the *viscous heating rate*

$$\Phi_V = \rho T \left.\frac{dS}{dt}\right|_V = \eta_{vis}\left(\frac{dv}{dz}\right)^2 \approx \frac{\eta_{vis}\Delta v^2}{L^2} \approx 1 \cdot 10^{-7} \quad , \tag{1.4}$$

and the *Joule heating rate*

$$\Phi_J = \rho T \left.\frac{dS}{dt}\right|_J = \frac{j^2}{\lambda_{el}} = \frac{c_L^2}{16\pi^2\lambda_{el}}(\nabla \times B)^2 \approx \frac{c_L^2\Delta B^2}{16\pi^2\lambda_{el}L^2} \approx 7 \cdot 10^{-5} \quad . \tag{1.5}$$

Here j is the current density and c_L the light velocity. For the *radiative heating rate* we have in the gray case

$$\Phi_R = \rho T \left.\frac{dS}{dt}\right|_R = 4\pi\overline{\kappa}(J - B) \tag{1.6}$$

where J is the frequency-integrated mean intensity, B the frequency-integrated Planck function and $\overline{\kappa}$ the gray Rosseland opacity, mainly due to the H^- ion, which can be approximated (with p the gas pressure) by

$$\frac{\overline{\kappa}}{\rho} = 1.38 \cdot 10^{-23} p^{0.738} T^5 \qquad cm^2/g \quad . \tag{1.7}$$

The heating rates (1.3) to (1.5) show that normally these processes are

z (km)	T (K)	ρ (g/cm^3)	c_S (cm/s)	v (cm/s)	l (cm)
0	6400	$2.7 \cdot 10^{-7}$	$8.3 \cdot 10^5$	$4.0 \cdot 10^{-5}$	$2.9 \cdot 10^{-2}$
500	4200	$6.0 \cdot 10^{-9}$	$6.7 \cdot 10^5$	$1.8 \cdot 10^{-3}$	1.1
1000	5900	$7.5 \cdot 10^{-11}$	$7.9 \cdot 10^5$	0.28	$1.1 \cdot 10^2$
1500	6400	$2.5 \cdot 10^{-12}$	$8.3 \cdot 10^5$	4.4	$3.3 \cdot 10^3$
2100	9200	$1.2 \cdot 10^{-13}$	$1.5 \cdot 10^6$	92	$1.0 \cdot 10^3$
2543	447000	$2.3 \cdot 10^{-15}$	$1.0 \cdot 10^7$	4800	$1.9 \cdot 10^6$

Table 1.1. *Temperature T, density ρ, sound speed c_S, wind velocity v and molecular mean free path l in the VAL81-C model as a function of height z.*

insufficient to balance the empirical chromospheric cooling rate of $-\Phi_R = 10^{-1} erg\ cm^{-3}\ s^{-1}$, determined from VAL81-C.

As the chromosphere exists on the Sun for billions of years, there should be steady state, and the left hand side of Eq. (1.2) must be zero. This can be seen from computing the entropy gradient $\partial S/\partial z \approx g/T$, where g is the solar gravity and v the solar wind flow speed, which from the solar mass loss rate of $\dot{M} = 10^{-14} M_\odot/y$ can be derived using $v = \dot{M}/(4\pi\rho R_\odot^2) \approx 1.1 \cdot 10^{-11}/\rho$ of which typical values are shown in Tab. 1.1. In this table also the mean free path $l \approx 1/(3 \cdot 10^{-16} n_H)$ is given, valid for non-ionized gas, with n_H the hydrogen number density.

In the chromosphere we thus find

$$\left.\frac{dS}{dt}\right|_R + \left.\frac{dS}{dt}\right|_M = 0 \quad , \tag{1.8}$$

which can be written

$$\frac{4\pi\overline{\kappa}}{\rho T}(J - B) + \left.\frac{dS}{dt}\right|_M = 0 \quad . \tag{1.9}$$

Conclusion: *In stellar chromospheres the main energy balance is between radiation and mechanical heating.*

In the special case of *radiative equilibrium* where there is no mechanical heating and the energy generated within the Sun is transported purely by a steady flow of radiation, one has $dS/dt|_M = 0$ and obtains $J = B$ (the absorbed radiative energy $\overline{\kappa}J$ is equal to the emitted radiative energy $\overline{\kappa}B$). With $J = \sigma T_{eff}^4/2\pi$, valid for the surface of a star, roughly represented by a black body of effective temperature T_{eff} (the factor 1/2 comes from the fact that at the solar surface there is only radiation going away from the star), and $B = \sigma T^4/\pi$, where σ is the Stefan-Boltzmann constant, one gets from Eq. (1.9) for the outer stellar layers the boundary temperature $T_b = 2^{-1/4} T_{eff} \approx 0.8\ T_{eff}$ For the Sun one has $T_{eff} = 5770\ K$ and

$T_b = 4600\ K$. This shows that in absence of mechanical heating we would expect to have temperatures of the order of the boundary temperature in the regions above the stellar surface.

However, as a chromosphere is a layer where the temperature is observed to rise in outward direction to values $T \gg T_{eff}$, it is clear that one must have $B \gg J$ and from Eq. (1.9) therefore $dS/dt|_M \gg 0$. This shows that *for chromospheres, mechanical heating is essential.* As for the transition layer and corona conductive and wind losses become important in addition to the radiative losses, and because these combined losses cannot be balanced by thermal conduction from a reservoir at infinity, but must ultimately be supplied from the stellar interior, there is an even stronger conclusion: that *for the existence of chromospheres and coronae, mechanical heating is essential.*

Moreover, chromospheres and coronae can only be maintained if mechanical heating is supplied *without interruption.* The time scale, in which the excess chromospheric temperature will cool down to the boundary temperature if the mechanical heating were suddenly disrupted, is given by the *radiative relaxation time* for which we have

$$t_{Rad} = \frac{\Delta E}{-\Phi_R} = \frac{\rho c_v \Delta T}{16\overline{\kappa}\sigma T^3 \Delta T} = \frac{\rho c_v}{16\overline{\kappa}\sigma T^3} \approx 1.1 \cdot 10^3\ s \quad . \tag{1.10}$$

Here ΔE is the heat content of the gas element, c_v the specific heat, and typical chromospheric values have been used. It is seen that in timescales of a fraction of an hour the chromosphere would cool down to the boundary temperature if mechanical heating would suddenly stop.

How can mechanical heating processes be visualized? From Eqs. (1.3) to (1.5) it is seen that these terms would only become significant compared to the observed radiative cooling rate $-\Phi_R$, if the length scale L is considerably decreased. For acoustic waves as well as longitudinal MHD tube waves, this is accomplished by *shock formation*, where the temperature jump occurs over the very short molecular mean free path l (see Tab. 1.1). For magnetic cases, by the formation of *current sheets*, where the magnetic field jumps occur over very small distances. In summary one can conclude that shock waves and current sheets are efficient mechanical heating mechanisms. For the corona (and possibly in the magnetic chromosphere at high altitude) additional heating mechanisms, like e.g. the dissipation of high-frequency gyrokinetic plasma waves operate (Marsch, Vocks & Tu 2001).

1.4 Overview of the heating mechanisms

Table 1.2 gives an overview of the mechanisms which are thought to provide a steady supply of mechanical energy to balance the chromospheric and

energy carrier	*dissipation mechanism*
hydrodynamic heating mechanisms	
acoustic waves, P<P_A	shock dissipation
pulsational waves, P>P_A	shock dissipation
magnetic heating mechanisms	
1. alternating current (AC) or wave mechanisms	
slow mode mhd waves, longitudinal mhd tube waves	shock dissipation
fast mode mhd waves	Landau damping
Alfvén waves (transverse, torsional)	mode-coupling resonance heating compressional viscous heating turbulent heating Landau damping
magnetoacoustic surface waves	mode-coupling phase-mixing resonant absorption
2. direct current (DC) mechanisms	
current sheets	reconnection (turbulent heating, wave heating)

Table 1.2. *Proposed chromospheric heating mechanisms*

coronal losses (for an extensive review of heating mechanisms see e.g. Narain & Ulmschneider 1996). The term *heating mechanism* comprises three physical aspects, the *generation* of a carrier of mechanical energy, the *transport* of mechanical energy into the chromosphere and corona and the *dissipation* of this energy.

Table 1.2 shows the various proposed energy carriers which can be classified into two main categories as *hydrodynamic* and *magnetic* heating mechanisms. Both the hydrodynamic and the magnetic mechanisms can be subdivided further according to frequency. Acoustic waves are high frequency hydrodynamic fluctuations with periods $P < P_A$ and pulsational waves have periods $P > P_A$. Here P_A is the acoustic cut-off period

$$P_A = \frac{4\pi c_S}{\gamma g} \quad , \tag{1.11}$$

where c_S is the sound speed, g the gravity and $\gamma = 5/3$ the ratio of specific

heats. A typical value for the acoustic cut-off period for the Sun ($g = 2.74 \cdot 10^4\ cm/s^2$, $c_S = 7\ km/s$) is $P_A \approx 190\ s$.

The magnetic mechanisms are subdivided into high frequency wave- or *AC (alternating current)-mechanisms* and current sheet- or *DC (direct current)-mechanisms* where one has time variations of low frequency. Also in Tab. 1.2 the mode of dissipation of these mechanical energy carriers is indicated.

Ultimately the mechanical energy carriers derive their energy from the nuclear processes in the stellar core from where the energy is transported by radiation and convection to the stellar surface. In late-type stars the mechanical energy generation arises from the gas motions of the surface convection zones. These gas motions are largest in the regions of smallest density near the top boundary of the convection zone. Due to this, the mechanical energy carriers, particularly the acoustic and MHD waves, are generated in a narrow surface layer.

1.5 Search for the important heating mechanisms

Although the heating mechanisms listed in Tab. 1.2 are known to work in terrestrial applications, the question is, which of these will operate in the solar or stellar situations and particularly, what are the major mechanisms which generate chromospheres. Because the Sun is so close to Earth compared to other stars one might think that this question can be decided by solar observations. Actually we are extremely lucky when we resolve spatial structures of 0.1 arc sec on the Sun, that is, linear scales of 70 km which is much bigger than the shock structure which is of the size of a molecular mean free path l (see Tab. 1.1) or the current sheet thickness which have sizes in the m range.

For many years it was therefore not possible to decide whether the main heating mechanism of the solar chromosphere is acoustic waves or rather an unresolved magnetic mechanism. It is very surprising that only by observing distant stars, which are mere point sources on the celestial sphere, could this question be definitively decided. The reason for this is, that stars differ in four basic parameters from the Sun: metallicity Z_M, effective temperature T_{eff}, gravity g and rotation period P_{Rot}, and that these differences have a large influence on the acoustic and magnetic wave generation.

a. Acoustic heating

All late-type stars have surface convection zones, and every turbulent flow field generates acoustic waves. Propagating down the steep density gradient (see Tab. 1.1) of the stellar surface layers the acoustic waves suffer rapid

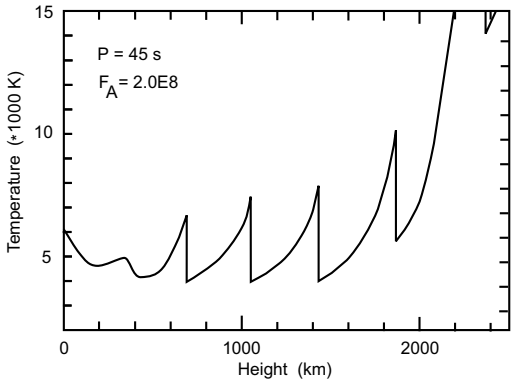

Fig. 1.2. Temperature distribution for a monochromatic acoustic wave with period $P = 45\ s$ and initial acoustic flux $F_A = 2.0 \cdot 10^8\ erg\ cm^{-2}s^{-1}$ in the solar atmosphere.

amplitude growth due to wave energy flux conservation. With the velocity amplitude v the wave energy flux is given by $F_{\rm A} = \rho v^2 c_{\rm Ph}$, where $c_{\rm Ph}$ is the propagation speed which is close to the sound speed, $c_{\rm S}$. Despite of strong radiation damping an amplitude growth $v \propto {\rm e}^{z/2H}$ occurs due to the exponential density decrease. As the wave crests of large amplitude waves move faster than the wave troughs, shocks form which develop a sawtooth shape and typically have velocity amplitudes $v < c_{\rm S}$. The shocks convert the wave energy into heat. This is called *acoustic heating theory*. The heating comes from the entropy jump ΔS at the shock front,

$$\Phi_M = \rho T \left.\frac{dS}{dt}\right|_M = \frac{\rho T}{P} \Delta S \quad , \tag{1.12}$$

where P is the period of the sawtooth wave into which the acoustic wave develops.

Figure 1.2 shows a radiatively damped monochromatic acoustic wave with a period $P = 45\ s$ and an initial acoustic flux $F_A = 2.0 \cdot 10^8\ erg\ cm^{-2}s^{-1}$ in the solar atmosphere. It is seen that the wave amplitude $\Delta T \sim \Delta v$ grows rapidly with height. But the actual growth is not so rapid because of radiation damping, which removes wave energy (and thus decreases the amplitude) by radiation losses. The amplitude growth at about 500 km causes shock formation and the wave subsequently grows into a sawtooth wave. Here the shock-jump dissipates the wave energy according to Eq. (1.12). It is seen that the shock-jumps become similar in size, independent of height. This is the so-called '*limiting shock strength*' behaviour which is common for monochromatic waves in gravitational atmospheres. The magnitude of this

temperature jump depends only on the wave period P and it can be shown that the dissipation of such waves can balance the observed chromospheric radiation losses (Ulmschneider 1990, 1991).

When in a time-dependent situation a shock moves through a gas element, the entropy jump ΔS introduced to the gas by the wave gets subsequently radiated away until the next shock comes along. If the next shock arrives before the gained thermal energy has been completely radiated away, then the gas element gets hotter after each shock. This rise of the temperature in the gas element continues until a stage is reached, where the entropy jump ΔS is completely radiated away at the moment where the next shock arrives. This state is called *dynamical equilibrium* and in this stage the mean chromospheric temperature distribution becomes time-independent. Together with the attainment of a high mean chromospheric temperature, the distribution of mass (the density) adjusts to the new scale height and to the support by the wave pressure imparted by the shocks (Gail, Cuntz & Ulmschneider 1990).

Note that monochromatic acoustic waves were chosen for the purpose of demonstrating the limiting strength behavior of shocks. In reality, the waves heating the chromosphere comprise a wide spectrum that stretches from the acoustic cutoff frequency (5 mHz) to large values (>60 mHz); the upper limit is set by radiation damping in the layers in the convection zone where the waves are generated. Monochromatic waves are more a feature of chromospheric dynamics.

Lighthill (1952) and Proudman (1952) have shown in terrestrial applications, that for free turbulence (away from any solid boundaries) one has quadrupole sound generation, in which the generated sound depends on the eighth power of the turbulent velocity. These authors have derived the expression

$$F_A = \int 38 \frac{\rho u^8}{c_S^5 H} dz \quad , \tag{1.13}$$

called *Lighthill-* or *Lighthill-Proudmann formula*, where $H = \Re T/\mu g$ is the scale height. Here u is the convective velocity (obtained for stars using a convection zone code), $\Re$ is the gas constant and μ is the the mean molecular weight, with $\mu = 1.3$ for the unionized solar gas. This Lighthill-formula has been well tested and confirmed in terrestrial applications.

Based on convection zone models and using the so-called Lighthill-Stein theory (see Musielak et al. 1994), Ulmschneider, Theurer & Musielak (1996) have computed acoustic energy fluxes F_A ($erg\ cm^{-2}s^{-1}$) for a wide range of late-type stars as shown in Fig. 1.3. This figure shows that because of

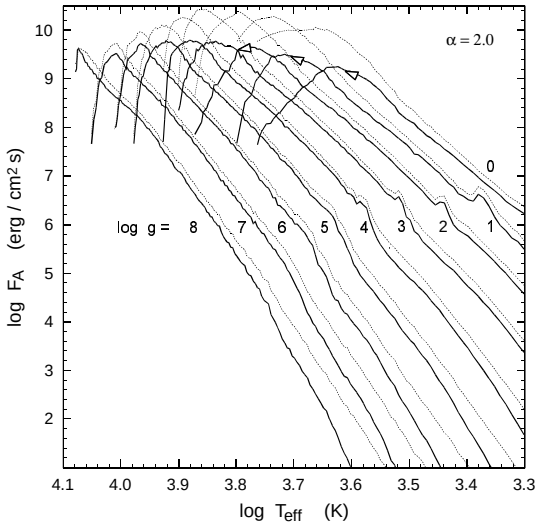

Fig. 1.3. Acoustic fluxes F_A (solid) for stars versus T_{eff} for given $\log g$ and mixing length parameter $\alpha = 2.0$. Also shown (dotted) are acoustic fluxes derived from the Lighthill-formula (1.13)

the u^8-dependence, F_A varies greatly with T_{eff} and g and that Eq. (1.13) despite of its simplicity gives quite reasonable results. That F_A also varies strongly with metallicity Z_M, particularly for cool stars where the opacity is not dominated by atomic hydrogen, has been shown by Ulmschneider et al. (1999). Yet F_A is independent of the rotation period P_{Rot} because the convection zones do not depend on rotation.

These acoustic fluxes and the wave periods derived from the acoustic spectra provided by the Lighthill-Stein theory can now be used to compute the propagation of the waves into the outer stellar atmosphere. This way theoretical chromosphere models (Fig. 1.2) of non-magnetic stars or stellar regions are created. On basis of these models it is possible to compute the emission cores of the main chromospheric lines, the Ca II H and K as well as Mg II h and k lines, and evaluate the total theoretical Ca II and Mg II emission fluxes in these lines. Buchholz et al. (1998) were the first to show that *these theoretical line fluxes agreed quite well with the lower boundary of the observed emission fluxes in these lines, called basal flux line.* This basal flux line is indicated in Fig. 1.4 by the dashed curve and fits the data of the stars with minimum emission flux.

That calculations, *starting from first principles* by using only the three parameters Z_M, T_{eff} and g, produced such a nice agreement with the purely

observational basal flux line showed that *the acoustic wave heating must be a basic mechanism of stellar chromospheres.*

b. Magnetic wave heating

Let us now turn to the non-magnetic regions of the chromosphere. Solar observations show that appart from sunspots and plage regions most of the magnetic flux occurs in small flux tubes with a diameter of about a scale height at the solar surface (e.g., Stenflo 1978, Solanki 1993). It has been observed, that the turbulent flows of the convection zone strongly perturb these magnetic tubes and generate magnetic waves. Squeezing the tubes generates *longitudinal mhd tube waves*, shaking produces *transverse tube waves* and twisting *torsional tube waves.* If the turbulent flows of the convection zone by the generation of acoustic waves provide a basic heating mechanism for the chromosphere, could the generation of magnetic waves by the same flows not give us a basic heating mechanism for magnetic regions? Here again stellar observation give the strongest evidence.

Vaughan & Preston (1980), Noyes et al. (1984) and others discovered that the greater the observed emission flux deviates from the basal flux line, the more rapidly the star rotates, and the more extensively it is covered by magnetic fields. Unfortunately a solar and stellar *dynamo theory* which would allow to predict the magnetic field coverage upon specification of the four basic parameters is presently not available. But by replacing the fourth parameter P_{Rot} by an assumed *filling factor of the magnetic field at the stellar surface* f, the heating of magnetic chromospheres can be studied independently of the dynamo theory. The filling factor is the ratio of the surface area covered by magnetic fields to the total surface area.

We assume that stars are fully covered with a forest of magnetic flux tubes, similar to those on the Sun, which at the stellar surface have a diameter equal to the scale height and a magnetic field strength $B_0 = 0.85 B_{eq}$ where $B_{eq} = \sqrt{8\pi p_0}$ and p_0 is the gas pressure outside the tube. The cross section of these tubes increases with height and at the canopy height fill out the entire available space. Ulmschneider, Musielak & Fawzy (2001) as well as Musielak & Ulmschneider (2001, 2002) have computed longitudinal and transverse wave energy fluxes for a large number of late-type stars on basis of such tubes.

For different filling factors f, stars with different magnetic flux tube forests can be constructed. The magnetic wave fluxes and wave periods can be used to compute the propagation of longitudinal waves along these flux tubes. Here the transverse wave flux is assumed to augment the longitudinal wave flux by mode-coupling while the atmosphere outside the flux tubes

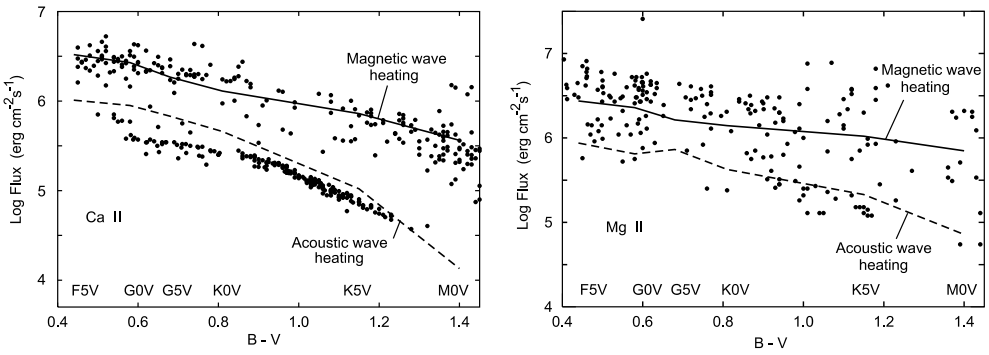

Fig. 1.4. Total observed Ca II H+K (left)and Mg II h+k line core emission fluxes of minimum flux stars and active dwarfs are shown as dots, compared with theoretical fluxes for pure acoustic wave heating and for magnetic wave heating in flux tubes, with an area filling factor of f=0.4, after Fawzy et al. (2002b).

is heated by acoustic waves. Again the core emission fluxes of the Ca II and Mg II lines emerging from the stars covered by a flux tube forest can be calculated and compared with observations. For this we evaluate the radiative transfer along many ray paths through the tube forest taking into account contributions from magnetically and acoustically heated regions. Figures 1.4 show results by Fawzy et al. (2002a, b). It is seen that by varying the filling factor from the case f=0 for pure acoustic heating to f=0.4 (mainly magnetic wave heating) appears to account for the observed variation of the chromospheric emission in Ca II, and most of the variation in Mg II. Yet for the Mg II emission, which occurs at greater height in the chromosphere than Ca II, there seems to be a gap between our results for f=0.4 and the largest observed emission. This indicates that although magnetic wave heating appears to be the main heating mechanism for most of the magnetic chromosphere, at the highest chromosphere an additional non-wave heating mechanism, presumably reconnective microflare heating appears to operate (Fawzy et al. 2002b).

1.6 Summary and outlook

The basic physical process which generates the solar chromosphere and that of other late-type stars is mechanical heating of which the main heating processes can now be identified. The base of the chromosphere is heated by pure acoustic shock waves, the lower and middle chromosphere with an increasing importance of the magnetic flux tubes are heated by longitudinal magnetohydrodynamic shock waves propagating in the vertically oriented

flux tubes which spread with height and eventually fill out all the available space. In the high chromosphere one very likely has an additional non-wave magnetic heating mechanism, possibly (reconnective) microflare heating.

Continuous heating by a wide spectrum of acoustic waves as well as intermittent heating by isolated shocks are permitted, but the observed cooling requires sustained, continuous heating. This excludes the model proposed by Carlsson & Stein (1994), where a shock heats the chromosphere once every three minutes provided there is a wave, and does not heat for the longer periods implied by the filling factor of 50% (Carlsson, Judge & Wilhelm 1997) of the oscillating part of the chromosphere (Kalkofen, Ulmschneider & Avrett 1999, Kalkofen 2001).

There remains the question of *what limits the chromospheres at the bottom and at the top.* The lower boundary is the temperature minimum. In cool stars, shock formation occurs at these heights and initiates the chromospheric temperature rise. For hot stars the growth of the generated shocks is delayed by strong radiation damping and the chromospheric temperature rise commences only after the zone of strong damping has been passed. The top boundary of the chromosphere occurs, when the main radiative cooling mechanisms (Lyα, Ly continuum and Mg II h+k cooling) at the high temperature end of the chromosphere cease to work because of complete ionization. In this case the heating becomes unbalanced and the temperature quickly rises up to coronal values.

References

Anderson, L. S. & Athay, R. G. 1989, ApJ 336, 1089

Avrett, A. H. 1985, in: Chromospheric Diagnostics and Modelling, B. W. Lites, ed., Sacramento Peak, 67

Buchholz, B., Ulmschneider, P., Cuntz, M. 1998, ApJ, 494, 700

Carlsson, M., Judge, P. G. & Wilhelm, K. 1997, ApJ 486, L63

Carlsson, M. & Stein, R. F. 1994, in Chromospheric Dynamics, Proc. Mini-Workshop, Inst. Theor. Astroph., Oslo, 47

Edlén B. 1941, Ark. mat., astr.och fys. 28 B, No.1

Fawzy D., Rammacher W., Ulmschneider P., Musielak Z.E., Stępień K. 2002a, A&A, subm.

Fawzy D., Ulmschneider P., Stępień K., Musielak Z.E., Rammacher W. 2002b, A&A, subm.

Fleck, B., Domingo, V. & Poland, A. I. 1995, The SOHO Mission, Kluwer Academic Publ., Boston

Fontenla, J. M., Avrett, E. H. & Loeser, R. 1993, ApJ 406, 319

Gail H.-P., Cuntz M., Ulmschneider P. 1990, A&A, 234, 359

Grotrian W. 1939, Naturwiss. 27, 214

Kalkofen, W. 2001, ApJ 557, 376

Kalkofen, W., Ulmschneider, P. & Avrett, E. H. 1999, ApJ 521, L141

Lighthill, M. J., 1952, Proc. Roy. Soc. London A211, 564

Marsch E., Vocks C., Tu C.-Y. 2001, Nonlin. Proc. in Geophys. 10, 1

Musielak Z.E., Rosner R., Stein, R.F., Ulmschneider P. 1994, ApJ 423, 474

Musielak Z.E., & Ulmschneider P. 2001, A&A 370, 541

Musielak Z.E., & Ulmschneider P. 2002, A&A, in press

Narain U., Ulmschneider P. 1996, Space Sci Rev. 75, 453

Noyes R.W., Hartmann L.W., Baliunas S.L., Duncan D.K., Vaughan A.H., 1984, ApJ 279, 763

Proudman I., 1952, Proc. Roy. Soc.London, A214, 119

Skumanich, A., Smythe, C. & Frazier, E.N. 1975 ApJ 200, 747

Solanki S.K. 1993, Space Sci. Rev., 63, 1

Stenflo, J.O. 1978, Rep. Prog. Phys. 41, 865

Stenflo, J.O. 1994, Solar Magnetic Fields, Kluwer, Dordrecht

Ulmschneider P. 1990, in: Cool Stars, Stellar Systems and the Sun, Astr. Soc. Pacific Conf. Ser. 9, G. Wallerstein, Ed., p. 3

Ulmschneider, P. 1991, in Mechanisms of Chromospheric and Coronal Heating, P. Ulmschneider, E. Priest and R. Rosner, eds., Springer Verl., Berlin, 328
Ulmschneider P., Musielak Z.E., Fawzy D.E. 2001, A&A 374, 662
Ulmschneider P., Theurer J., Musielak Z.E. 1996, A&A 315, 212
Ulmschneider P., Theurer J., Musielak Z.E., Kurucz R. 1999, A&A 347, 243
Vaughan A.H., Preston G.W. 1980, PASP 92, 385
Vernazza J.E., Avrett E.H., Loeser R., 1981, ApJ Suppl. 45, 635